J Geod (2007) 81:703–712
DOI 10.1007/s00190-007-0137-1

ORIGINAL ARTICLE

Correcting superconducting gravity time-series using rainfall modelling at the Vienna and Membach stations and application to Earth tide analysis

Bruno Meurers · Michel Van Camp · Toon Petermans

Received: 8 March 2006 / Accepted: 16 January 2007 / Published online: 14 February 2007

Abstract We demonstrate the possibility to improve the signal-to-noise ratio of superconducting gravity time-series by correcting for local hydrological effects. Short-term atmospheric events associated with heavy rain induce step-like gravity signals that deteriorate the frequency spectrum estimates. Based on 4D modeling constrained by high temporal resolution rain gauge data, rainfall admittances for the Vienna and Membach superconducting gravity stations are calculated. This allows routine correction for Newtonian rain water effects, which reduces the standard deviation of residuals after tidal parameter adjustment by 10%. It also improves the correction of steps of instrumental origin when they coincide with step-like water mass signals.

Keywords Gravity time-series · Tidal analysis · Rain water effect modeling · Superconducting gravity

1 Introduction

To look for temporal gravity changes, gravity time-series have to be corrected for known contributions like tidal, polar and atmospheric effects. Performing tidal analysis also requires correction for the atmospheric pressure variations, which affect gravity differently depending on their frequency (e.g., Warburton and Goodkind 1977; Crossley et al. 1995). Usually, the barometric effects (loading and mass attraction) are accounted for by using a linear admittance factor. This factor, around $-3.5\,\mathrm{nms}^{-2}/\mathrm{hPa}$ in the spectral range of short-periodic tides, is station-dependent, varies from gravity record to record, and is determined using a barometer at the gravity station.

However, this correction is not satisfactory during local short-term variations and extreme events like thunderstorms or the passage of cold fronts, as short-term atmospheric pressure variation of a few hPa can induce steep gravity decreases of a few nms^{-2} within 10 min to an hour (Müller and Zürn 1983; Meurers 2000). Moreover, rainfall also plays an essential role (e.g., Francis et al. 2004).

Recently, hydrological effects on gravity have been investigated by numerous authors (for a summary of these investigations, see Van Camp et al. 2006). Rainfall data based on cumulative hourly or daily samples have been frequently used for interpreting temporal gravity variations (e.g., Bower and Courtier 1998; Imanishi 1999; Kroner 2002; Harnisch and Harnisch 2006). However, to the best of our knowledge, a standard correction based on high temporal resolution rainfall data (1 min samples) has never been applied routinely to process gravity time-series spanning several years.

This is the aim of this paper. We investigate 10 years of data from the superconducting gravimeter (SG) at Vienna, Austria, and two years from the SG at Membach, Belgium. At Vienna, 123 rain events have been analyzed, and 48 at Membach. We show that step-like gravity drops are mostly caused by gravity effects due

B. Meurers (✉)
Institute of Meteorology and Geophysics, University Vienna, Althanstrasse 14, 1090 Wien, Austria
e-mail: bruno.meurers@univie.ac.at

M. Van Camp · T. Petermans
Royal Observatory of Belgium, Seismology, Avenue Circulaire, 3, 1180 Bruxelles, Belgium
e-mail: mvc@oma.be

T. Petermans
e-mail: toon.petermans@oma.be

to rainfall or vertical air mass redistribution without air pressure variation, or a combination of both.

The observed gravity drop is of physical origin and should not be eliminated blindly during data processing. On the other hand, step-like signals deteriorate the frequency spectrum estimates and tidal analysis from SG data. This paper demonstrates the successful application of water gravity effect models applied routinely to improve the signal-to-noise ratio of SG time-series and in particular, the tidal analysis results at Membach and Vienna.

2 4D water gravity effect modeling

Water gravity effect modeling is very sensitive to the shape of the topography. It is also important to consider that water is drained immediately on impermeable areas like buildings. The SG in Vienna is installed on the basement floor of a large building, whose cross section and the horizontal position of the SG sensor are known in detail. This station is located on a gentle topographic slope and the surface close to the station is well above the SG (Fig. 1a, b). However, this does not hold for the distant terrain. Therefore, the gravity effect of mass distributed above and below the station partly compensates each other (Fig. 2).

The rainfall sensor (tipping bucket type, 0.1 mm resolution) providing 1 min data is situated about 20 m from the SG. At Membach, the SG is installed 48 m below the surface. Topography is moderate at Membach too, but the SG is below the topographic surface almost everywhere surrounding the station (Fig. 1c, d). The rain gauge (tipping bucket type, 0.1 mm resolution) is located at the entrance of the gallery, 140 m away from the SG.

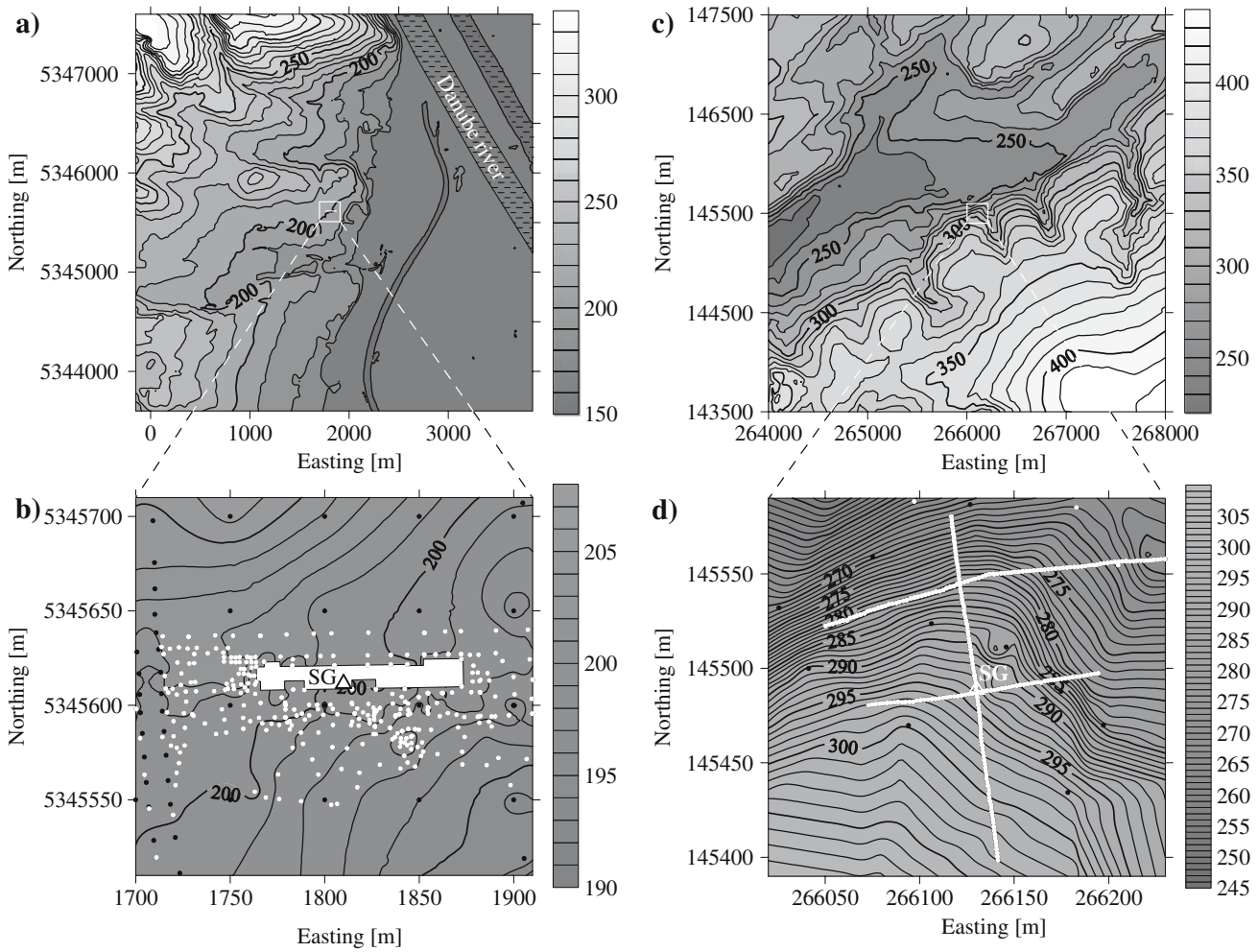

Fig. 1 Topography [m] in the vicinity of the SG stations Vienna (**a, b**) and Membach (**c, d**). SG sensor elevations: 192 m (Vienna) and 244 m (Membach). *Black dots*: DEM data, *white dots*: local geodetic survey. The blanked area in (**b**) represents the building section where no rainfall water is stored in the soil

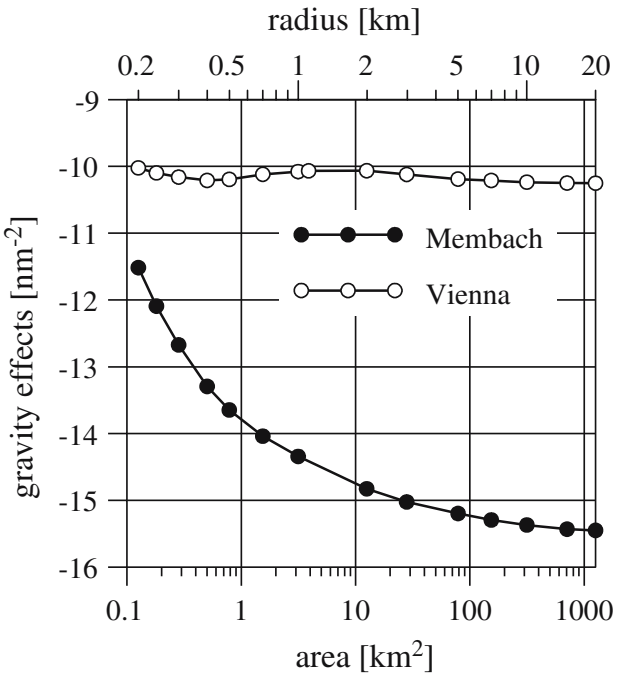

Fig. 2 Gravitational effect of a circular water layer (thickness 40 mm) centered on the SG sensor for different radii. At Vienna, the gravity effect does not much vary with the extension of the contributing mass due to compensation effects of distant layer parts. At Membach, the layer is situated above the SG sensor almost everywhere

Modeling of the rain water mass is based on the following assumptions:

- Rain water intrudes into the uppermost soil layer and remains there. This is justified for a period of a couple (1 to 2) of hours after the rainfall, as evapotranspiration is a slow process compared with charge due to heavy rain and thus is not yet effective;
- No run-off except on impermeable areas, where water drains into the sewage system;
- Rainfall is equal in the station surroundings;
- No surface deformation due to the water mass.

Consequently, the water mass is modeled as layer of constant thickness. Upper and lower boundaries of this layer are approximated by polyhedral surfaces defined by Delaunay triangulation (e.g., Renka 1996) of digital elevation models (DEM). At Vienna, the DEM is based on a regular grid with 50 m spacing. Irregularly distributed height data spaced by less than 10 m on average has been supplemented by local geodetic surveying within the close surrounding of the SG (Fig. 1b). At Membach, we used a DEM with average spacing of about 30 m and local data surveyed along profiles above the gallery (Fig. 1d). At both stations, the DEM covers a circle of at least 20 km radius centered at the SG. The corresponding gravity effect is calculated using the method of Götze and Lahmeyer (1988) (Fig. 2).

To separate hydrological and atmospheric effects in the SG data, the temporal behavior of the model must be known. As rainfall data in high temporal resolution are available at the SG stations only, we added the following suppositions (Fig. 3):

- The rain cell approaches the station with constant velocity $\boldsymbol{v}$;
- Each location ($\boldsymbol{x}$) touched by the rain cell exhibits the same cumulative rainfall function $\mathrm{rwh_S}(t)$ as that observed at the SG site ($\boldsymbol{x}_\mathrm{S}$);
- Plain rain cell front of limited extension Y centered at the SG.

The cumulative rainfall function $\mathrm{rwh_S}(t)$ at the SG site is defined by

$$\mathrm{rwh_S}(t) = \sum_{j=-n(t)}^{0} r(t + j\,\delta t) \qquad n(t) = \frac{t - t_0}{\delta t} \tag{1}$$

In Eq. (1), r denotes the rainfall sampled in time intervals δt and t_0 the time when rainfall of a given event starts. Then, the cumulative rain water $\mathrm{rwh}(\boldsymbol{x}, t)$ at any location $\boldsymbol{x}$ and at time t equals

$$\mathrm{rwh}(\boldsymbol{x}, t) = \begin{cases} 0 & p(\boldsymbol{x}, t) < 0 \\ \mathrm{rwh_S}\left(\frac{p(\boldsymbol{x},t)}{|\boldsymbol{v}|}\right) & p(\boldsymbol{x}, t) \geqslant 0\ ,\ q(\boldsymbol{x}, t) \leqslant \frac{Y}{2} \end{cases} \tag{2a}$$

with

$$p(\boldsymbol{x}, t) = \frac{\boldsymbol{v} \cdot (\boldsymbol{x}_\mathrm{S} - \boldsymbol{x})}{|\boldsymbol{v}|} + |\boldsymbol{v}|(t - t_0)$$
$$q(\boldsymbol{x}, t) = \sqrt{\left|(\boldsymbol{x}_\mathrm{S} - \boldsymbol{x}) + \boldsymbol{v}(t - t_0) - \boldsymbol{v}\frac{p(\boldsymbol{x}, t)}{|\boldsymbol{v}|}\right|^2} \tag{2b}$$

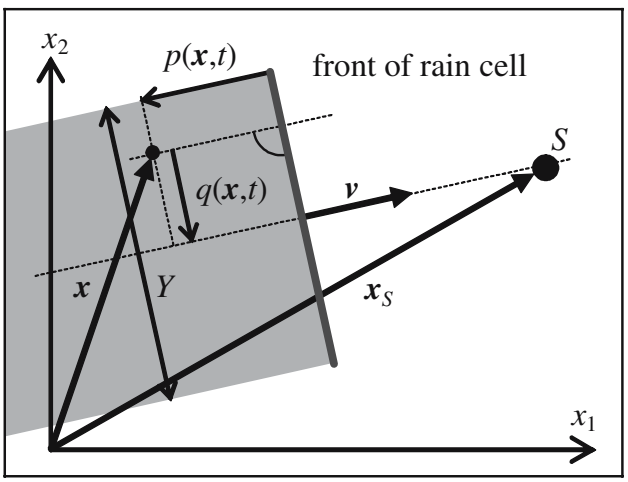

Fig. 3 Description of the 4D model parameter

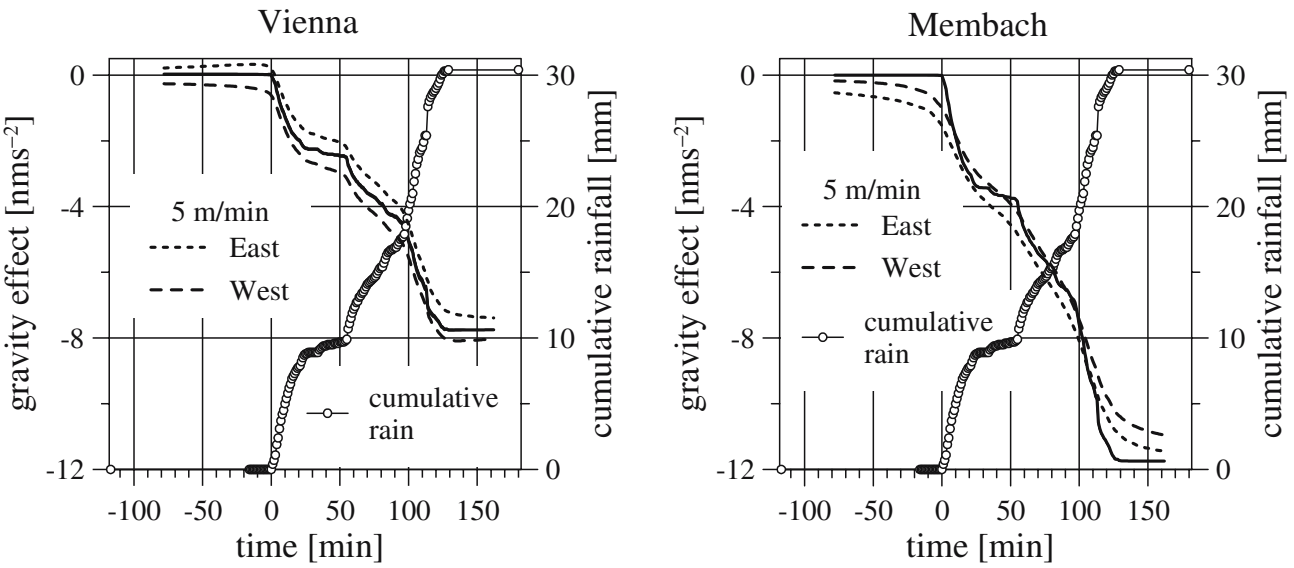

Fig. 4 Gravitational effect of a rain cell approaching from different directions and with different velocities. Almost no differences are visible for realistic velocities (e.g. 500 m/min, *solid lines*) while only for extremely low velocities (e.g. 5 m/min) the result depends of the direction from where the rain cell approaches (*dashed lines*)

Figure 4 compares the model results for Vienna and Membach based on 1-min rainfall data. The velocity and the direction from where the rain cell is approaching plays a minor role for realistic velocities (a few 100 m/min), because the water mass in the close vicinity of the station dominates. Only in the rare cases where the velocity is extremely low, very small differences can be observed (dashed lines in Fig. 4). The rainfall admittance converges rapidly (Fig. 5a), which justifies to model the gravity effect of rain by a single admittance, which might not be the case for other stations with uneven topography.

The 4D modeling provided the following rainfall admittances: Vienna: $-0.254\,\mathrm{nms}^{-2}/\mathrm{mm}$ and Membach: $-0.386\,\mathrm{nms}^{-2}/\mathrm{mm}$. These numbers agree well with the linear least-squares (LSQ) fit of Fig. 5b, which displays the gravity residual drop magnitude as function of cumulative rain for each rain event. Figure 5b demonstrates that the ratio between gravity change and amount of water per rain event is stable without seasonal features.

The a priori rainfall correction can now easily be implemented by subtracting the cumulative rainfall according to Eq. (1), multiplied by the rainfall admittance, from the raw calibrated 1-min SG data. In this case, t_0 in Eq. (1) denotes the start time of the SG data series. Based on these results, the meteorological influences on gravity were investigated.

Typical case studies are shown in Fig. 6. The results of the 4D model are represented in the bottom panels of Fig. 6 by grey lines. In Fig. 6a, the model reflects the step due to cumulative rainfall correctly. However, heavy rain starts significantly later than the gravity drop indicating that additional atmospheric processes like air mass redistribution may play an important role. This event was associated with heavy thunderstorms. Figure 6b and c refer to case studies where the cumulative rainfall effect does not fit the gravity drop, while in Fig. 6d the model almost perfectly matches the observation.

At Membach, 76% of the gravity drops were explained by the rain water effect alone, like in Fig. 6d, while at Vienna, the model fitted perfectly only 58% of all rain events. However, even in the other cases, where rainfall is involved, the water mass model was able to explain the dominant part of the gravity drops like in Fig. 6a. These drops coincided with rainfall in 85% of the cases at Vienna and 91% at Membach.

For those events where the rain model does not perfectly explain the gravity drop (e.g., Fig. 6a, b, c), additional meteorological processes are involved. The standard air pressure correction fails if the atmosphere violates the hydrostatic equilibrium assumption like in events associated with vertical convection. The Newtonian effect of vertical air mass redistribution may contribute essentially.

A change of the vertical air density structure does not necessarily cause air pressure variations, but can induce gravitational effects (Meurers 2000; Simon 2002). In numerous cases, the sharp drop of gravity coincides exactly with that of air temperature (Fig. 6a, b, c), indicating that air mass exchange and/or vertical redistribution contributes to the observed gravity signal. Modeling

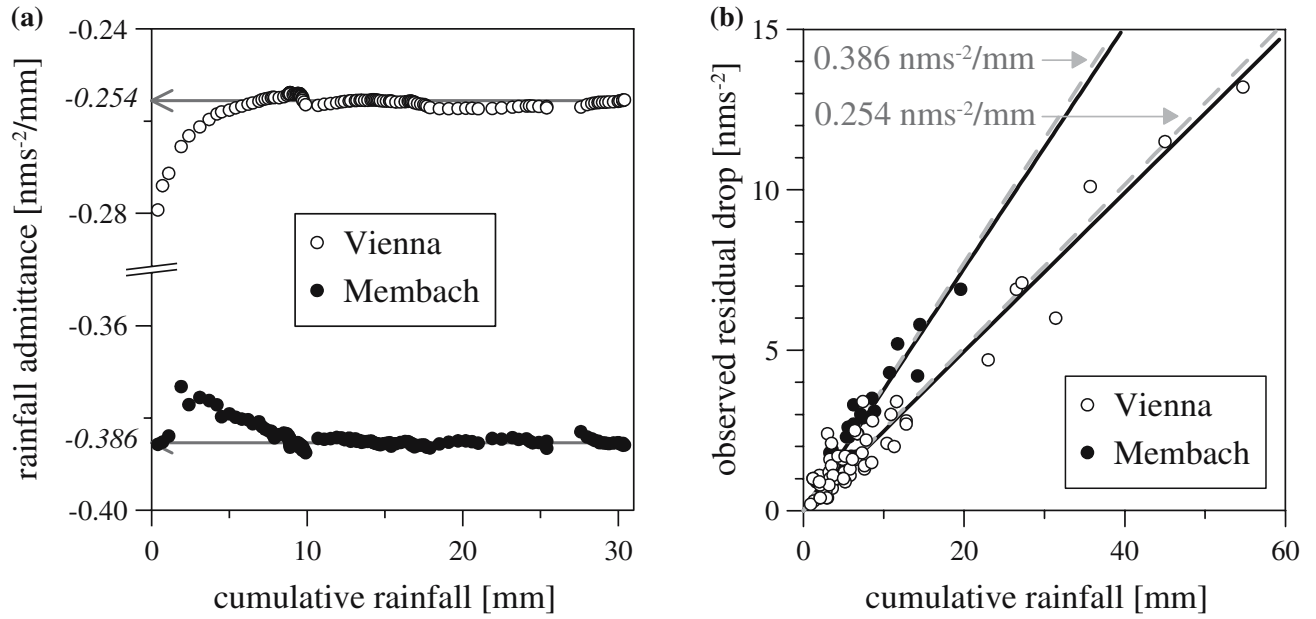

Fig. 5 **a** Rainfall admittance as function of cumulative rain for the 4D model (rain cell approaching from West with velocity of 500 m/min) used in Fig. 4. **b** Observed gravity residual drop magnitude in relation to cumulative rain and LSQ fit (*solid lines*). *Dashed lines* represent the rainfall admittance factors obtained from the 4D model in Vienna and Membach respectively

of these processes suffers from the lack of meteorological data in high temporal and spatial resolution; but this should be a future perspective. At present, only simplistic models can be considered.

3 Tidal analysis improvement

The following investigation shows how tidal analysis results can be improved when the rainfall admittance model is applied to the SG data. Both Vienna and Membach data were analyzed without and with an a priori rainfall correction. During data preprocessing, only steps due to known instrumental causes were removed. In the case of rainfall correction, the gravity effect of cumulative rain was calculated by applying the rainfall admittance and subtracted from the raw 1-min data as previously described. Afterwards, the 1-min data was decimated to 1-h samples and analyzed by applying the ETERNA v3.3 package (Wenzel 1996). The SG time-series cover 3554 days at Vienna and 871 days at Membach.

The standard deviation of the gravity residuals after tidal parameter adjustment is reduced by about 10% when the rainfall effect is corrected (Vienna: from 0.547 to 0.504 nms^{-2}, Membach: from 0.730 to 0.667 nms^{-2}). Amplitude factor changes are in the order of 10^{-3} or less, phase lags change by 10^{-3} to 10^{-2}. These variations are slightly lower than the standard deviation of the adjusted parameters; they are therefore not statistically significant.

However, it is worth mentioning that the amplitude factors of high amplitude tidal waves (O_1, P_1, K_1, S_1) and even Ψ_1 and Φ_1 show similar variations in Vienna and Membach. The changes are rather small, but perhaps have influence on the accuracy of free core nutation parameter determination. As expected, generally the tidal parameter variation is less in the semidiurnal (SD) than in the diurnal (D) frequency bands.

It has to be proven that the reduction of the standard deviation is actually due to cleaning the raw data with respect to the rain effect. This is shown by analyzing the 1-min gravity residuals obtained without and with a priori rainfall correction. Another analysis is applied on the 1-h residuals obtained from the tidal analysis adjustment. First, for the Vienna time-series, the 1-min gravity residuals (obtained after detiding and air pressure correction using the single admittance concept) have been analyzed within 6-h windows, which have been centered at heavy rain events associated with a sharp gravity residual drop. For each event, the root-mean-squared (RMS) gravity residual obtained after rainfall correction has been determined and subtracted from that without correction.

Figure 7 shows a pronounced linear relationship between the differences of the RMS gravity residuals

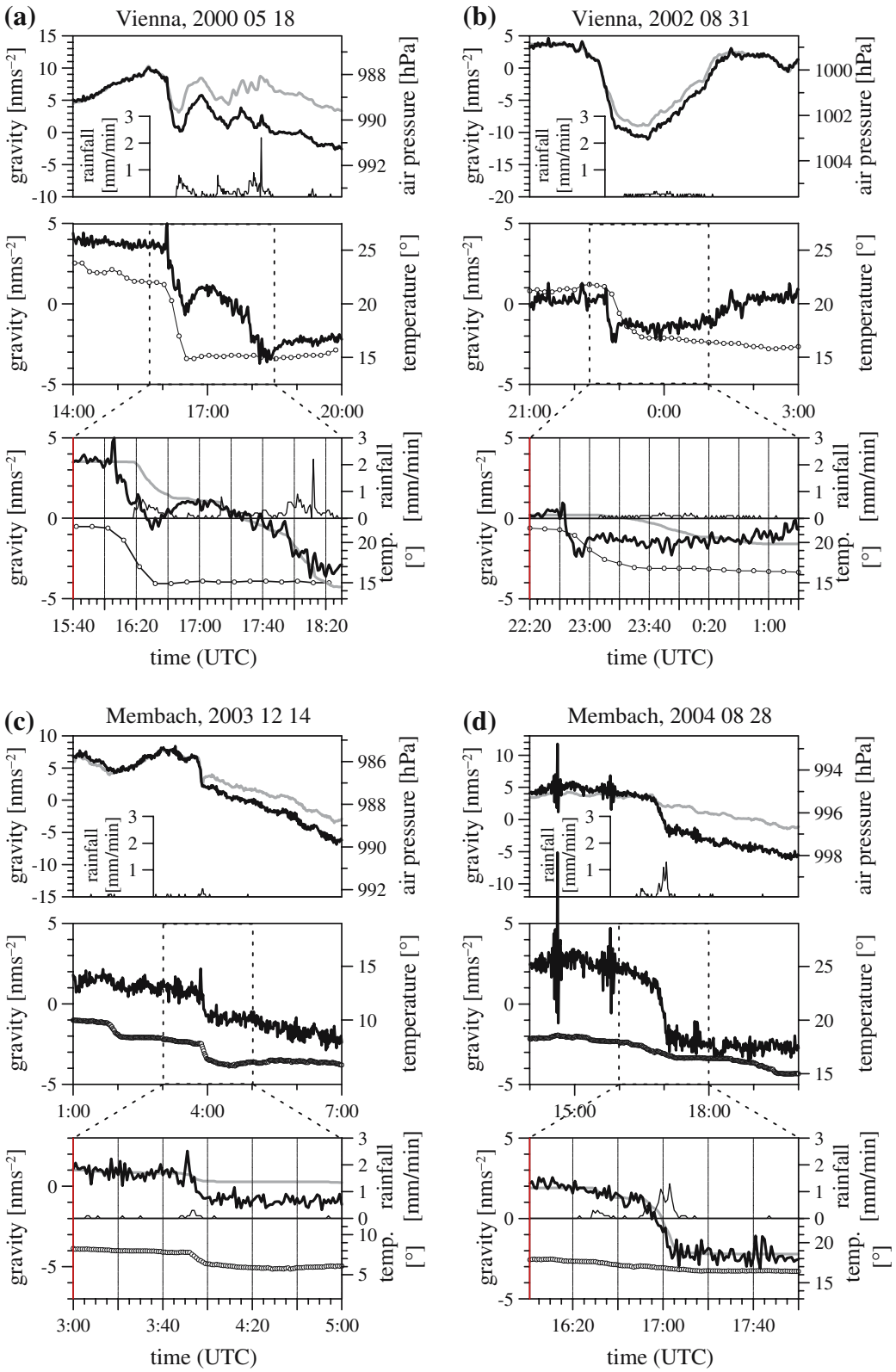

Fig. 6 Gravity variations caused by different meteorological processes. *Top*: air pressure (*grey*), tide free gravity measurements (*black*) and rainfall (*thin line*). *Middle*: gravity (*black*) corrected from the air pressure effect [admittance factor: $-3.53\,\mathrm{nms}^{-2}/\mathrm{hPa}$ (Vienna) and $-3.32\,\mathrm{nms}^{-2}/\mathrm{hPa}$ (Membach)] and air temperature (*dots*). *Bottom*: exaggerated section of the middle panel, water mass effect (*grey*), 1 min rainfall samples (*thin line*)

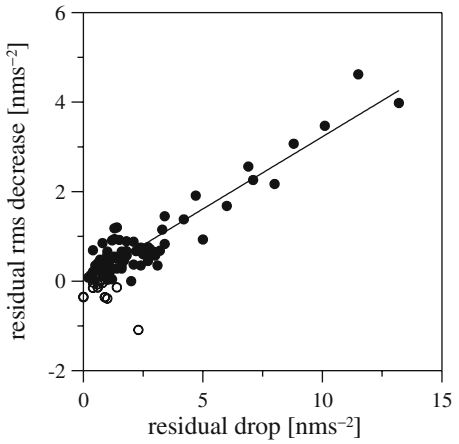

Fig. 7 Differences between the root-mean-squared 1-min gravity residuals as function of the residual drop magnitude for all heavy rain events at Vienna. For each meteorological event associated with a sharp gravity residual drop the root-mean-squared gravity residual obtained after rainfall correction has been determined within a 6-h window and subtracted from that without correction. *Open circles* indicate rare events where a background residual increase induced by unknown environmental effects compensates the rainfall effect

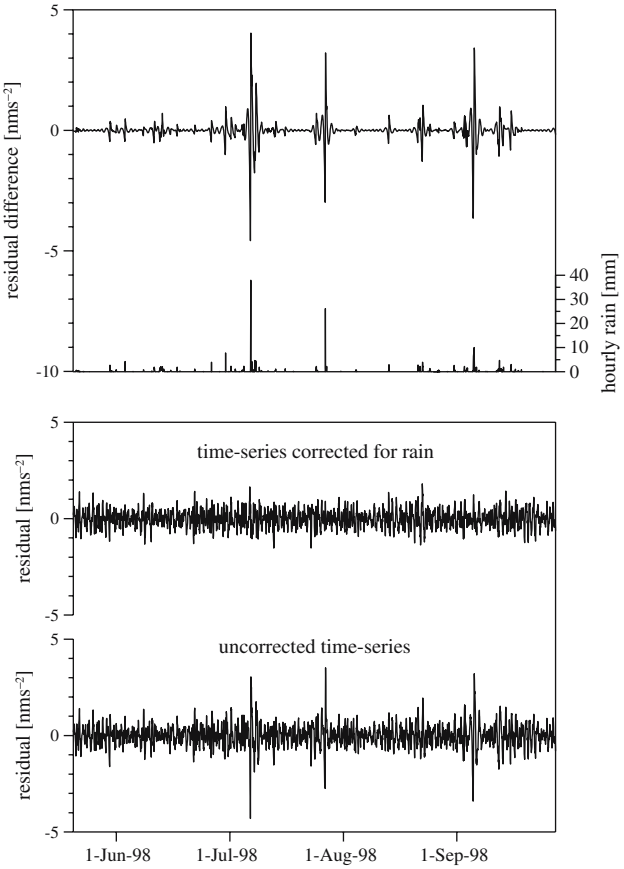

Fig. 8 Difference (*top panel*) between the hourly residuals (*bottom panel*) resulting from the tidal analysis of the gravity data with and without a priori rain effect correction respectively, and hourly rainfall

and the residual drop magnitude. Only when the residuals exhibit a strong background increase within the window interval, e.g., due to imperfectly corrected air pressure or unknown environmental effects, the rain signal may compensate the trend, and thus rainfall correction may even increase the RMS residual. In such rare cases, negative differences of the RMS gravity residuals have been observed (open circles in Fig. 7).

Figure 7 proves the effectiveness of the rainfall correction, which is additionally demonstrated by analyzing the structure of the residuals obtained from the tidal analysis of the 1-h data. Figure 8 shows the difference between the hourly residuals resulting from the tidal analysis of the gravity data with and without a priori rain effect correction. The differences are close to zero except in the immediate vicinity of rain events, where they show typical distortions expected to occur in the residuals if uncorrected steps are present. This holds even for events with little rain fall. As shown in the bottom panel of Fig. 8, the oscillations only appear in the residuals of the uncorrected time-series.

The rainfall admittance model used here does not take discharge processes into account, e.g., due to run-off or evaporation, which destroys the long-term drift information. This should not significantly influence tidal analysis results as long as only the D and SD bands are adjusted. To check this influence, the rain water model of Eq. (1) was extended according to Eq. (3) by assuming fast run-off after the rain fall event and much slower evapotranspiration effects.

$$\mathrm{rwh_S}(t) = \sum_{j=-\infty}^{0} r(t + j\,\delta t)\frac{1}{2}\left(\mathrm{e}^{j\,\delta t/\alpha} + \mathrm{e}^{j\,\delta t/\beta}\right) \tag{3}$$

Again, t is the time and $\delta t = 1$ min the sampling interval of the rainfall r. The discharge parameters $\alpha = 12$ h accounts for fast run-off and $\beta = 720$ h for slow evapotranspiration.

As expected, the tidal analysis results did not change significantly, neither the standard deviation (0.503 nms^{-2} at Vienna, 0.668 nms^{-2} at Membach), nor the tidal parameter variations in the D and SD bands.

The rainfall admittance concept based on the model according to Eq. (3) explains gravity anomalies after strong rainfall (Fig. 9) and reflects the instantaneous response of gravity to rain water. In contrast, models taking slow recharge processes into account that are exponential functions of time (e.g., Crossley et al. 1998; Harnisch and Harnisch 2002; Francis et al. 2004) do not fit the fast gravity drop immediately starting with rain.

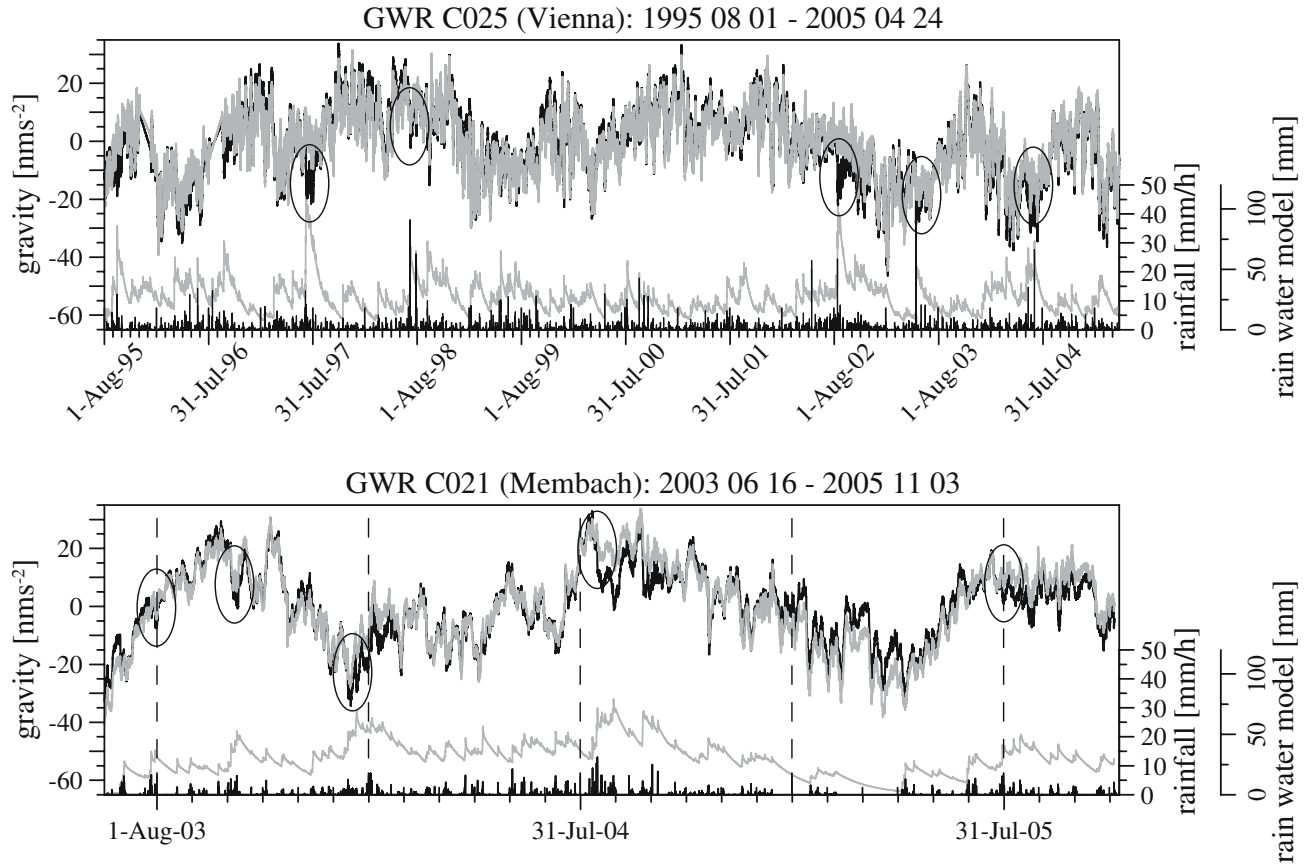

Fig. 9 Gravity in Vienna and Membach obtained by applying (*grey*) or not applying (*black*) the rain water mass model (*light grey*, *thin line*) based on the rainfall admittance (4D model) and discharge model (Eq. (3)). Rainfall data is displayed in *black*. The rain water mass model explains strong distortions after heavy rain fall events and long term rain fairly well (e.g. Vienna: 07/1997, 07/1998, 08/2002, 05/2003, 07/2004; Membach: 08&10/2003, 01&08/2004)

4 Application of the rain admittance model in data pre-processing

Generally, the instrumental drift is determined by absolute gravity (AG) observations at more or less regular intervals. However, correcting for SG steps is more difficult: unless several AG data are available just before and after the step, this procedure does not allow for correcting the steps at the nm/s^2 level.

Therefore, it may be helpful to correct the data for steps of known origin independently of AG measurements by checking the residuals. For instance, SG maintenance work or power supply interrupts can produce steps in gravity recordings. As already done with the air pressure admittance, the rainfall admittance model can be applied in order to help in discriminating instrumental steps from actual decrease in gravity due to meteorological influences.

A synthetic simulation (Fig. 10) demonstrates how the drift-free gravity residuals are potentially influenced if a real gravity signal is blindly removed together with instrumental steps. Assume a linear SG instrumental drift properly modeled using regular AG measurements (e.g., Van Camp and Francis 2006). Let an instrumental step occur in the middle of the time-series just at the same time as a step-like downward drop (10 nms^{-2}) due to rain, which is followed by an exponential discharge signal lasting over half a year.

After both step like features have been removed by any common step detection procedure, the rain-induced step superimposes the linear drift after the decay of the discharge signal. Consequently, an apparent drift with slightly higher drift rate than that of the true drift is estimated by the LSQ adjustment. This would not happen if the gravity drop due to rain had not been eliminated.

Therefore, a remove-restore technique is proposed: before looking for steps, the cumulative rain signal must be removed by applying the rainfall admittance model, as already done for the atmospheric pressure. After correcting instrumental steps, the rainfall model effect is restored.

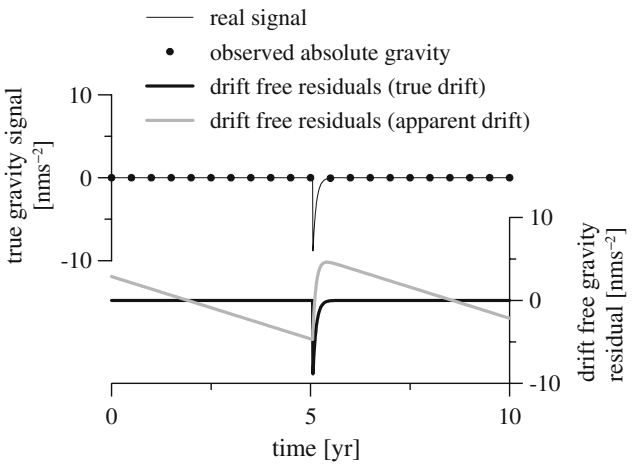

Fig. 10 Simulation of the influence of wrong step determination on drift free gravity residuals. If real step like signals are eliminated, the drift free residual (*grey*) does no longer recover the true gravity signal (*black*)

Figure 11 demonstrates a case study using observed SG data from Membach (09 October 2004). Heavy rain occurred during some maintenance work, which induced a large step of 116 nms^{-2} (Fig. 11, top panel, black line). First, the step was removed by applying the pre-processing module *Tsoft* (Van Camp and Vauterin 2005) without considering the 2 nms^{-2} step due to the water

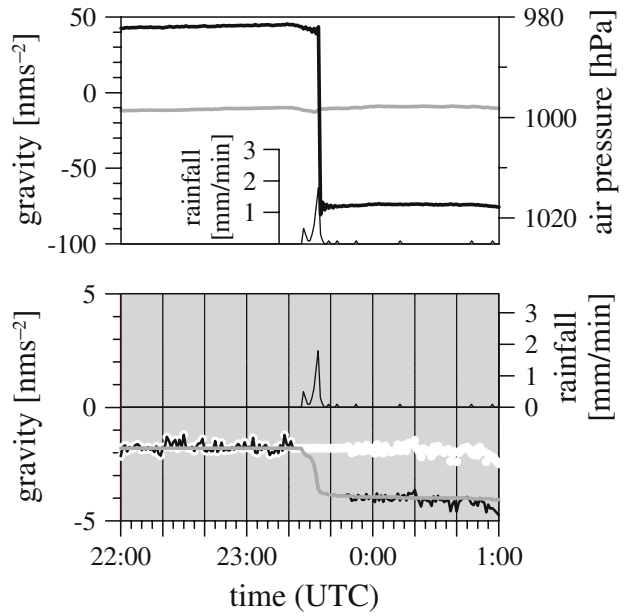

Fig. 11 Application of the rain water mass model for precise step determination (Membach 09 October 2004). *Top*: air pressure (*grey*), tide free gravity measurements (*black*) and rainfall samples (*thin line*). *Bottom*: gravity after removing the air pressure effect [admittance factor: −3.32 nms^{-2}/hPa] and after step correction (Tsoft) without (*white dots*) and with (*black line*) applying the proposed remove-restore technique. Water mass effect (*grey*), rainfall (*thin black line*).

mass effect (Fig. 11, bottom panel, grey line). Consequently the remaining gravity signal (Fig. 11, bottom panel, white dots) does not include the water mass effect. On the contrary, if the proposed remove-restore technique is applied, actual physical signals are kept in the gravity time-series (Fig. 11, bottom panel, black line), while pure instrumental artifacts are correctly removed.

5 Discussion and conclusions

We showed that the steep gravity decreases within 10 min to 1 h are associated with heavy rain starting at or up to 10 min later than the gravity drop. At Vienna, rainfall and gravity drop coincide in 85% of the cases (91% at Membach). Predominantly, the drops are connected with atmospheric processes of high vertical convection activity like thunderstorms, as gravity and air temperature are well correlated in most cases. The magnitude of the gravity drops depends on the total amount of rainfall accumulated during the event.

Step-like signals deteriorate the frequency spectrum estimates and tidal analysis. As the gravity drops are of physical origin, they should not be eliminated blindly, but corrected using water mass modeling constrained by high temporal resolution (1 min) rain data. As the influence of rain cell velocity is not significant, simple rainfall admittance models can be used. We calculated rainfall admittances for Vienna and Membach and showed that they are very dependent on the position of the SG sensor with respect to the local and near surrounding topography.

Correcting for rainfall effects reduces the standard deviation of the residuals after tidal parameter adjustment by 10%. From the metrological point of view, any method improving a signal-to-noise ratio is worth applying. Thus, SG data should be corrected whenever possible, even if there is no noticeable advance on the final tidal analysis results. Because the principle is simple, we propose to apply this method routinely on gravity time-series processing before starting step detection procedures.

As long as no long-period (>2 days) constituents are adjusted, the cumulative rainfall function defined in Eq. (1) combined with effective rainfall admittances can be used to calculate the water mass response. The gravitational effects due to air mass redistribution are not accounted for by this procedure, but this investigation showed that it is able to eliminate the dominant part of the residual drop.

For long-period constituents and proper interpretation of long-term gravity changes, hydrogeological investigations like those by Van Camp et al. (2006) should

be performed, because discharge processes like run-off, infiltration and evapotranspiration must be controlled by hydrogeological measurements. Even in case of gaps in rainfall data, hydrological data reflect the cumulative effects in contrast to data derived from rainfall observations alone.

Additionally, the rainfall admittance model is well suited to improve the correction of steps due to instrumental causes when they coincide with step-like signals originating from rain water mass.

Acknowledgements Cooperation with Geophysical and Climatological Divisions of the Central Institute for Meteorology and Geodynamics, Vienna, Austria, is gratefully acknowledged, as well as financial support by Austrian Science Foundation project P16480-GEO. The experience of Marc Vandiepenbeeck to test the rain gauge of Membach was greatly appreciated. We thank the reviewers, Tonie van Dam, Corinna Kroner, Yoichi Fukuda and Will Featherstone, for constructive comments and valuable suggestions which improved the paper considerably.

References

Bower DR, Courtier N (1998) Precipitation effects on gravity measurements at the Canadian absolute gravity site. Phys Earth Planet Int 106:353–369

Crossley D, Jensen O, Hinderer, J (1995) Effective barometric admittance and gravity residuals. Phys Earth Planet Int 90: 355–358

Crossley DJ, Xu S, van Dam T (1998) Comprehensive analysis of 2 years of SG data from Table Mountain, Colorado. In: Ducarme B, Pâquet P (eds) Proc. 13th Int. Symp. Earth Tides, Brussels, July 22–25, 1997, pp 659–668

Francis O, Van Camp M, van Dam T, Warnant R, Hendrickx M (2004) Indication of the uplift of the Ardenne in long term gravity variations in Membach (Belgium). Geophys J Int 158: 346–352

Götze HJ, Lahmeyer B (1988) Application of three dimensional interactive modeling in gravity and magnetics. Geophysics 53:1096–1108

Harnisch M, Harnisch G (2002) Seasonal variations of hydrological influences on gravity measurements at Wettzell. B Inf Marèes Terr 137:10849–10861

Harnisch M, Harnisch G (2006) Hydrological influences in long gravimetric data series. J Geodynamics 41:276–287

Imanishi Y (1999) Present status of SG T011 at Matsushiro, Japan. In: Ducarme B, Barthélemy J (eds) Proceedings of Workshop: "High Precision Gravity Measurements with Application to Geodynamics and Second GGP Workshop", Luxembourg, Cah Cent Eur Géodyn et de Séismol 17:97–102

Kroner C (2002) Zeitliche Variationen des Erdschwerefeldes und ihre Beobachtung mit einem supraleitenden Gravimeter im Geodynamischen Observatorium Moxa, Habilitationsschrift, Chemisch-Geowissenschaftliche Fakultät, FSU Jena, 149 pp

Meurers B (2000) Gravitational effects of atmospheric processes in SG gravity data. In: Ducarme B, Barthélemy J (eds) Proceedings of Workshop: "High Precision Gravity Measurements with Application to Geodynamics and Second GGP Workshop", Luxembourg, 1999, Cah Cent Eur Géodyn et de Séismol 17: 57–65

Müller T, Zürn W (1983) Observation of gravity changes during the passage of cold fronts. J Geophys 53: 155–162

Renka RJ (1996) ALGORITHM 751. TRIPACK: Constrained two-dimensional Delaunay Triangulation Package. ACM Trans Math Software 22(1): 1–8

Simon D (2002) Modelling of the field of gravity variations induced by the seasonal air mass warming during 1998–2000. B Inf Marées Terr 136:10821–10836

Van Camp M, Vauterin P (2005) Tsoft: graphical and interactive software for the analysis of time series and Earth tides. Comput Geosci 31(5):631–640

Van Camp M, Francis O (2006) Is the instrumental drift of superconducting gravimeters a linear or exponential function of time? J Geodesy: doi 10.1007/s00190-006-0110-4

Van Camp M, Vanclooster M, Crommen O, Petermans T, Verbeeck K, Meurers B, van Dam T, Dassargues A (2006) Hydrogeological investigations at the Membach station, Belgium, and application to correct long periodic gravity variations. J Geophys Res 111, B10403, doi:10.1029/2006JB004405

Warburton RJ, Goodkind JM (1977) The influence of barometric pressure variations on gravity. Geophys J R astr Soc 48: 281–292

Wenzel HG (1996) The nanogal software: Earth tide data processing package ETERNA 3.30. B Inf Marées Terr 124:9425–9439